Combination of lidar and model data for studying deep gravity wave propagation

Benedikt Ehard[1,2], Peggy Achtert[2,3], Andreas Dörnbrack[1], Sonja Gisinger[1], Jörg Gumbel[2], Markus Rapp[1,4] and Johannes Wagner[1,5]

[1] Deutsches Zentrum für Luft- und Raumfahrt (DLR), Institut für Physik der Atmosphäre, Oberpfaffenhofen, Germany [2] Department of Meteorology, Stockholm University, Stockholm, Sweden [3] Institute of Climate and Atmospheric Science, School of Earth and Environment, University of Leeds, Leeds, United Kingdom [4] Meteorological Institute Munich, Ludwig-Maximilians-Universität München, Munich, Germany [5] Institute of Meteorology and Geophysics Innsbruck, University of Innsbruck, Innsbruck, Austria

Correspondence: Benedikt.Ehard@dlr.de

EGU2015-10591

Motivation

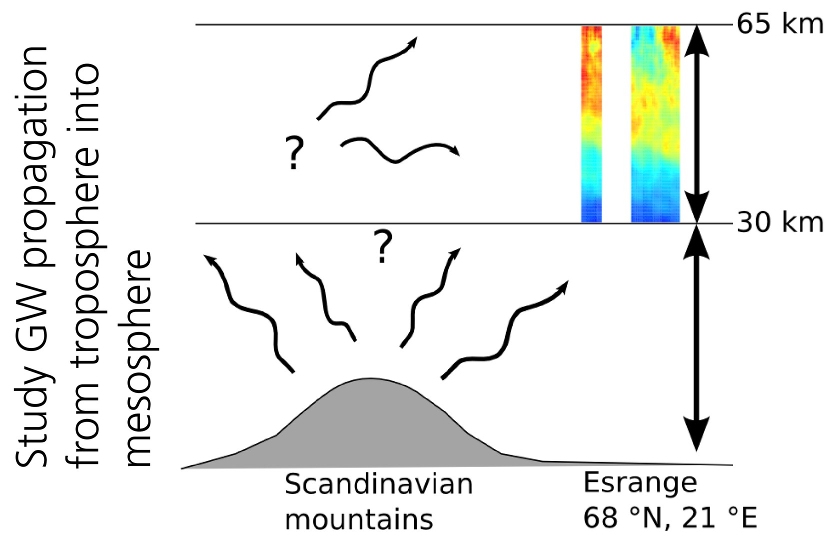

Rayleigh lidar temperature measurements by Esrange lidar

No Rayleigh temperature due to aerosols
→ use mesoscale simulations

Methodology

- Temperatures determined from the Esrange lidar's (68°N, 21°E) Rayleigh channel are combined with mesoscale simulations
- Advanced version of the Weather Research and Forecasting (WRF–ARW) model is used (Fig. 1)
- Temperature data is interpolated to the position of the Esrange lidar beam and averaged over the same time spans
- WRF temperature profiles below 30 km altitude are used to complete missing lidar measurements

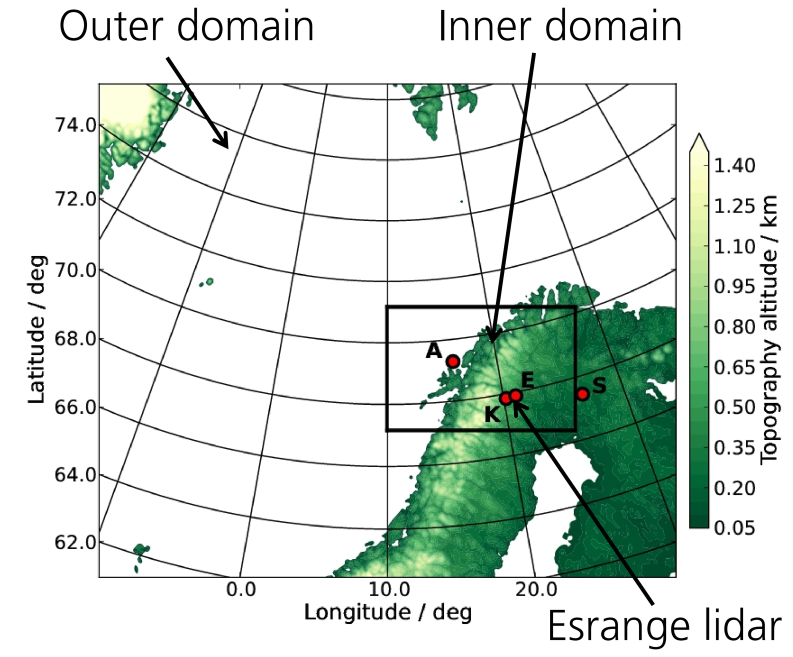

Fig. 1: Map of the domains used by the WRF model

WRF Validation

- WRF vs Radiosondes:
  Comparison of temperature perturbations T' determined from 21 radiosonde launches (Fig. 2):
  - Correlation coefficient: 0.912
  - Root-mean-square error: 0.97 K
- WRF vs Aircraft measurements:
  Comparison of 5s averaged Falcon in-situ temperature during 3 measurement flights:
  - Root-mean-square error: 0.53 K

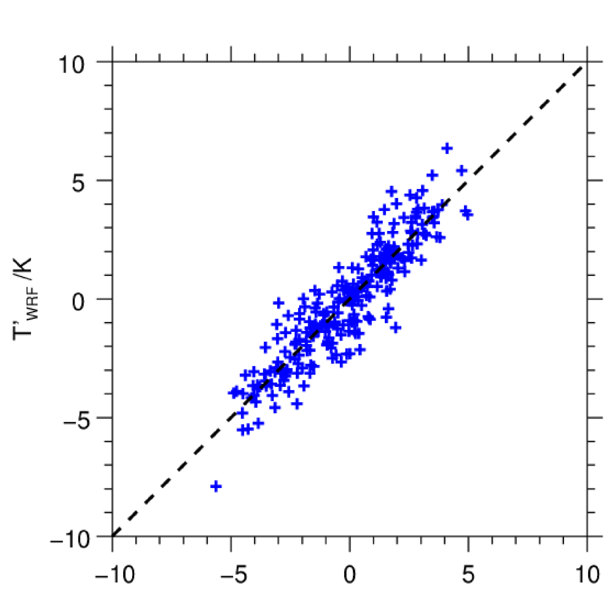

Fig. 2: Comparison of WRF and radiosonde temperature perturbations in 2 km wide altitude intervals

Wave Analysis for 3/4 December 2013

Vertical structure

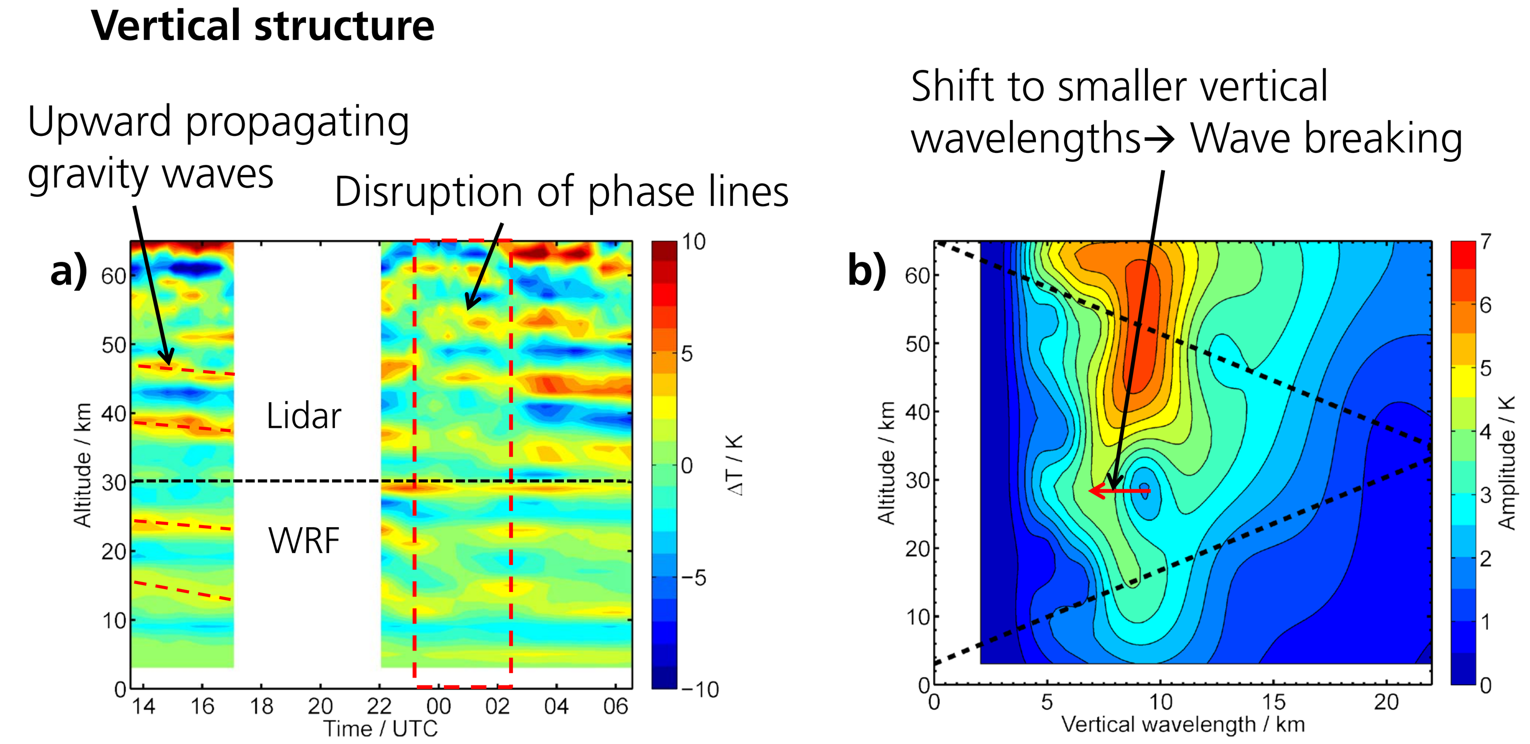

Fig. 3: a) Temperature perturbations from the combination of lidar measurements and WRF simulations at 3/4 December 2013; **b)** Corresponding mean wavelet spectrum

- Signatures of gravity waves throughout entire altitude region (Fig. 3a)
- Wave with dominant vertical wavelength ~9 km propagating from the tropopause region into the mesosphere (Fig. 3b)

Horizontal structure

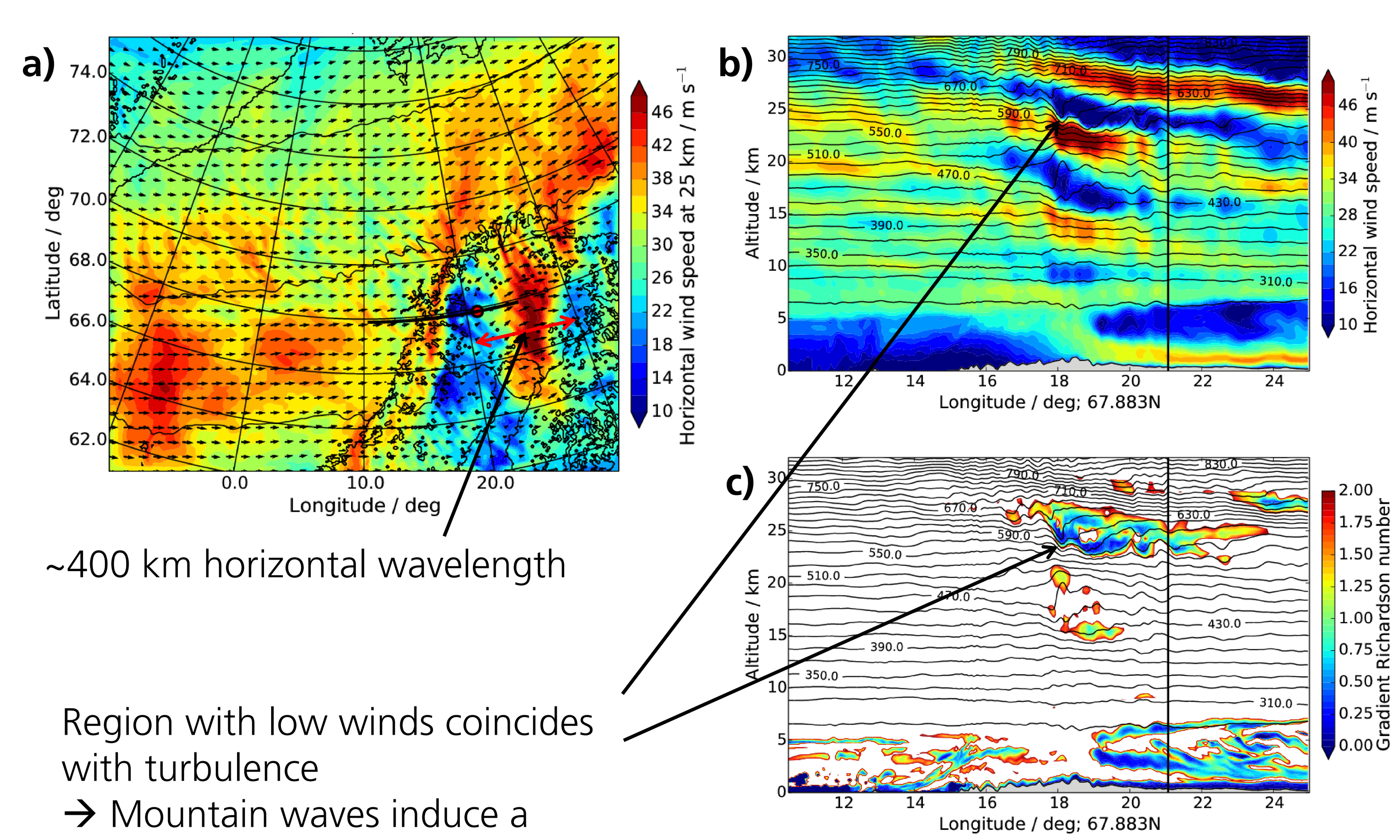

~400 km horizontal wavelength

Region with low winds coincides with turbulence
→ Mountain waves induce a critical layer
→ Leads to wave breaking

Fig. 4: Cross sections through the WRF model on 4 December 0100 UTC
a) horizontal wind speed at 25km altitude
b) horizontal wind speed along 67.883°N
c) horizontal wind speed along 67.883°N

Critical horizontal wavelength

- Calculated critical horizontal wavelength from Esrange radiosondes (Fig. 4)
  → Equal to vertical wavelength in case of hydrostatic mountain waves

Shift to smaller wavelengths

Similar to Fig. 3b) above 5 km altitude

→ Similarity between lidar spectrum and crit. hor. wavelength provides additional proof that the observed waves are hydrostatic mountain waves

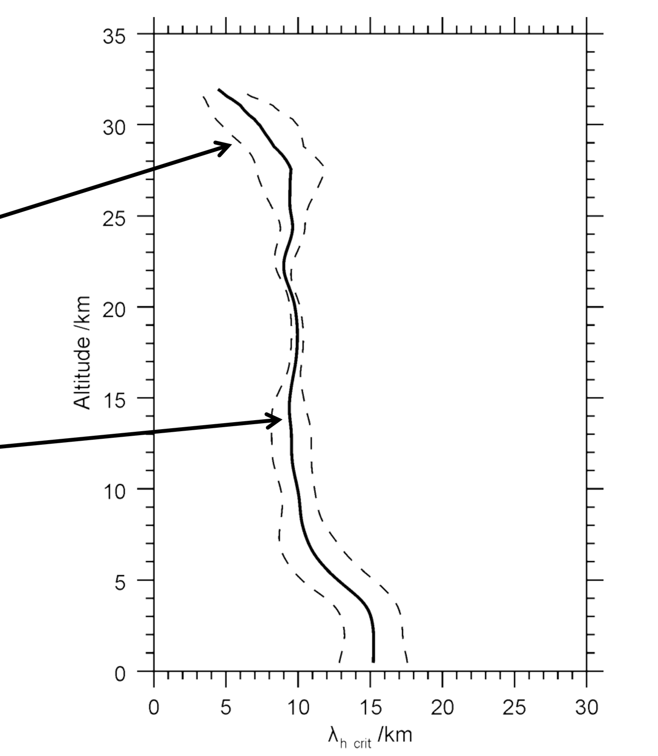

Fig. 5: Critical horizontal wavelength on 3/4 December 2013

Summary and Conclusion

- Missing lidar measurements below 30 km altitude were substituted by mesoscale simulations → enables studies of gravity wave propagation from the troposphere into the mesosphere
- WRF simulations show excellent agreement with local in-situ measurements
- Gravity wave with dominant vertical wavelength of ~9 km detected throughout the entire altitude range
- Wave breaking event around 25–30 km altitude captured by the WRF simulations
- Model fields and radiosonde observations suggest that observed waves are hydrostatic mountain waves

→ Observed deep gravity wave propagation from the troposphere into the mesosphere on 3/4 December 2013

Reference

- Ehard et al. (2015): Combination of lidar and model data for studying deep gravity wave propagation; *submitted to Mon. Wea. Rev.*